Agricultural and Forest Meteorology 297 (2021) 108248

Contents lists available at ScienceDirect

Agricultural and Forest Meteorology

journal homepage: www.elsevier.com/locate/agrformet

Assessing future drought risks and wheat yield losses in England

D Clarke [a], T M Hess [b], D Haro-Monteagudo [c], M.A. Semenov [d], J W Knox [b,*]

[a] NIAB TAG, Morley Business Centre, Norfolk, NR18 9DF, UK
[b] Cranfield University, Cranfield, Bedfordshire, MK43 0AL, UK
[c] Department of Geography, University of Aberdeen, Aberdeen AB24 3UF, UK
[d] Rothamsted Research, Harpenden AL5 2JQ, UK

ARTICLE INFO

Keywords:
Crop model
Sirius
drought indices
risk
wheat

ABSTRACT

Droughts pose a major risk to agricultural production. By comparing the outputs from an ecophysiological crop model (Sirius) with four drought severity indicators (DSI), a comparative assessment of the impacts of drought risk on wheat yield losses has been evaluated under current (baseline) and two future climate scenarios. The rationale was to better understand the relative merits and limitations of each approach from the perspective of quantifying agricultural drought impacts on crop productivity. Modelled yield losses were regressed against the highest correlated variant for each DSI. A cumulative distribution function of yield loss for each scenario (baseline, near and far future) was calculated as a function of the best fitting DSI (SPEI-5_{July}) and with the equivalent outputs from the Sirius model. Comparative analysis between the two approaches highlighted large differences in estimated yield loss attributed to drought, both in terms of magnitude and direction of change, for both the baseline and future scenario. For the baseline, the average year differences were large (0.25 t ha^{-1} and 1.4 t ha^{-1} for the DSI and Sirius approaches, respectively). However, for the dry year, baseline differences were substantial (0.7 t ha^{-1} and 2.7 t ha^{-1}). For the DSI approach, future yield losses increased up to 1.25 t ha^{-1} and 2.8 t ha^{-1} (for average and dry years, respectively). In contrast, the Sirius modelling showed a reduction in future average yield loss, down from a baseline 1.4 t ha^{-1} to 1.0 t ha^{-1}, and a marginal reduction for a future dry year from a baseline of 2.7 t ha^{-1} down to 2.6 t ha^{-1}. The comparison highlighted the risks in adopting a DSI response function approach, particularly for estimating future drought related yield losses, where changing crop calendars and the impacts of CO_2 fertilisation on yield are not incorporated. The challenge lies in integrating knowledge from DSIs to understand the onset, extent and severity of an agricultural drought with ecophysiological crop modelling to understand the yield responses and water use relations with respect to changing soil moisture conditions.

1. Introduction

Wheat is the most widely cultivated cereal globally, contributing 20% of total dietary calories consumed (Shiferaw et al., 2013). FAO (2017) reported that global crop production will need to increase 60% by the 2050s to support feed a larger, wealthier population. However, with limited scope for extending current cultivated areas, the emphasis will inevitably be on achieving significant increases in productivity (yield) to assure future food security (Reynolds et al., 2009). However, the current potential rates of yield increase will fall well below those needed to meet future food demands (Hall and Richards, 2013). Wheat is a temperate species, making conditions in western Europe, where seven of the ten highest wheat-yielding countries (including the UK) are located, particularly favourable (Kahiluto et al., 2019; Trnka et al., 2019). In 2018, 1.75 million hectares (40% of the arable area) in the UK were used for wheat production (Fig. 1); the average yield (7.8 t ha^{-1}) contributed to approximately 2% of global output, valued at £2.1 billion (Defra, 2018). However, a third of the UK wheat crop is grown on drought prone soils, resulting, on average, in a 10 to 20% loss in total production, valued at £72 million (Ober et al., 2011), but this can be considerably higher during drought years. For example, in 2018, despite a wet spring, average yields were negatively impacted due to the combination of sustained high temperatures and exceptionally low rainfall. Average yield in 2018 resulted in a 5.1% drop in total production from the previous year (Defra, 2018). The UK wheat industry perceives 'unpredictable weather' to be one of the highest risks to production (Ilbery

* Corresponding author
E-mail address: j.knox@cranfield.ac.uk (J.W. Knox).

https://doi.org/10.1016/j.agrformet.2020.108248
Received 4 April 2020; Received in revised form 3 November 2020; Accepted 11 November 2020
Available online 24 November 2020

et al., 2013) in combination with short intense periods of drought (Kendon et al., 2013).

Wheat is vulnerable to drought at many phenological stages, for example, drought can reduce germination and increase tiller death (Baker, 1989); water stress during stem extension and early booting stages (pollen development) can increase pollen sterility resulting in fewer grains and lower yields at maturity (Dodd et al., 2011). During the later stages in crop growth, drought can accelerate senescence resulting in lower grain numbers (during anthesis) and can cause the grain to inadequately fill (Trnka et al., 2014; AHDB, 2015). Marsh et al (2007) identified 12 'notable' and 6 'major' UK drought episodes spanning 35 years between 1912 and 2000, with a number of 'multi-year' drought events. The drought in 2018, followed by very dry spells in both 2019 and 2020 coupled with increasingly variable summer rainfall patterns has understandably raised questions regarding the impacts of short duration droughts on rainfed wheat yields in humid and temperate regions.

The onset, spatial extent and termination of droughts are very difficult to determine given that they are a creeping phenomenon and slow-onset hazard. Considerable effort has been dedicated to developing tools that provide an objective and quantitative evaluation of drought severity (Vicente-Serrano et al., 2012). These are often referred to as drought severity indices (DSIs) and are derived from meteorological or hydrological variables, including precipitation, evapotranspiration, streamflow, soil moisture or groundwater levels. They provide a value, or set of values, that can help describe the magnitude, duration, severity and spatial extent of droughts more easily than from raw data (Wilhite, 2005), form the primary tool for disseminating drought warnings and forecasts (Zargar et al., 2011) and constitute an integral part of drought monitoring and early warning systems in many countries.

Average UK wheat yields have been recorded since 1885, with some nationwide drought events causing noticeable yield reductions (Wreford and Adger, 2011) (Fig. 1). However, droughts that display a strong regional focus appear not to have affected national yields (for example, 2004 to 2006). It is thus difficult to provide a regional perspective on drought-yield relationships due to the limited temporal span of records. Although de-trending can remove some uncertainty (Vicente-Serrano et al., 2012), the reported steady increase in average yield (+1.2% yr^{-1}) (Shearman et al., 2005) over the 20th century (Fig. 1) means that the effects of drought can be masked. Losses due to drought can also be misinterpreted or hidden by yield reductions induced through other agronomic pressures such as lodging (Sterling et al., 2003), waterlogging, disease and pest outbreaks. The use of dynamic and process-based crop simulation models is currently the most widespread approach used for assessing the effects of increasingly variable weather including drought (Glotter and Elliot., 2016; Webber et al., 2018), as well as other agronomic and climatic factors, on food crop production (Ewert et al., 2015).

In the context of a national research effort to understand the impacts of droughts and water scarcity across a range of sectors including agriculture, this study aimed to assess the impacts of drought (expressed through water stress) on wheat yield under current and future climate conditions via two contrasting approaches; (i) evaluating drought risks on wheat by correlating selected DSIs with yield loss response functions and (ii) comparing the outputs from this regression driven modelling with equivalent yield losses derived from a complex ecophysiological crop model. The rationale was to better understand the relative merits and limitations of each approach from the perspective of agricultural drought impacts. DSIs are relatively simple to calculate and have been widely used by the water resources and hydrological modelling community, but their utility for understanding yield impacts has been limited. Crop models have been extensively used to evaluate yield responses to water and abiotic impacts, but they require local parameterisation. With the future frequency and intensity of droughts in the UK expected to increase (Burke and Brown, 2010; Burke et al., 2010; Rahiz and New, 2013), an improved understanding of the likely impacts and adaptation responses in cereal production are required. This study therefore has direct relevance to the wheat industry in terms of supporting improved approaches for future drought risk management, particularly given its economic importance as a commodity crop that is almost entirely dependent on rainfall for production. The highest intensity of wheat cropping in the UK is concentrated in central and eastern England (Fig. 2) in catchments that are already experiencing severe water resource stress (Knox et al., 2018). Adaptation strategies involving a switch from predominately rainfed to irrigated wheat production would therefore have major water resource implications.

2. Materials and methods

A long-term historical weather dataset (105 years) was compiled for a representative site (Cambridge) in eastern England, and used to derive four DSIs. An ecophysiological crop-growth model was then validated

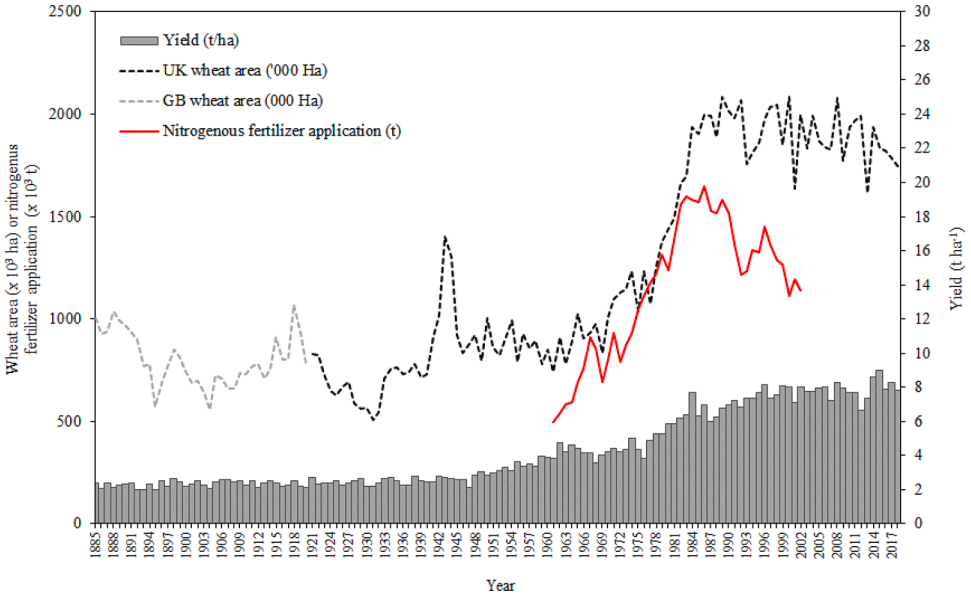

Fig. 1. Reported total wheat cropped area (ha^{-1}) in GB/UK between 1885 and 2018, UK total nitrogenous fertiliser application (t) (1961 to 2002) and average UK wheat yield (t ha^{-1}), 1885 to 2018 (Source: Defra, 2019; FAOSTAT, 2017).

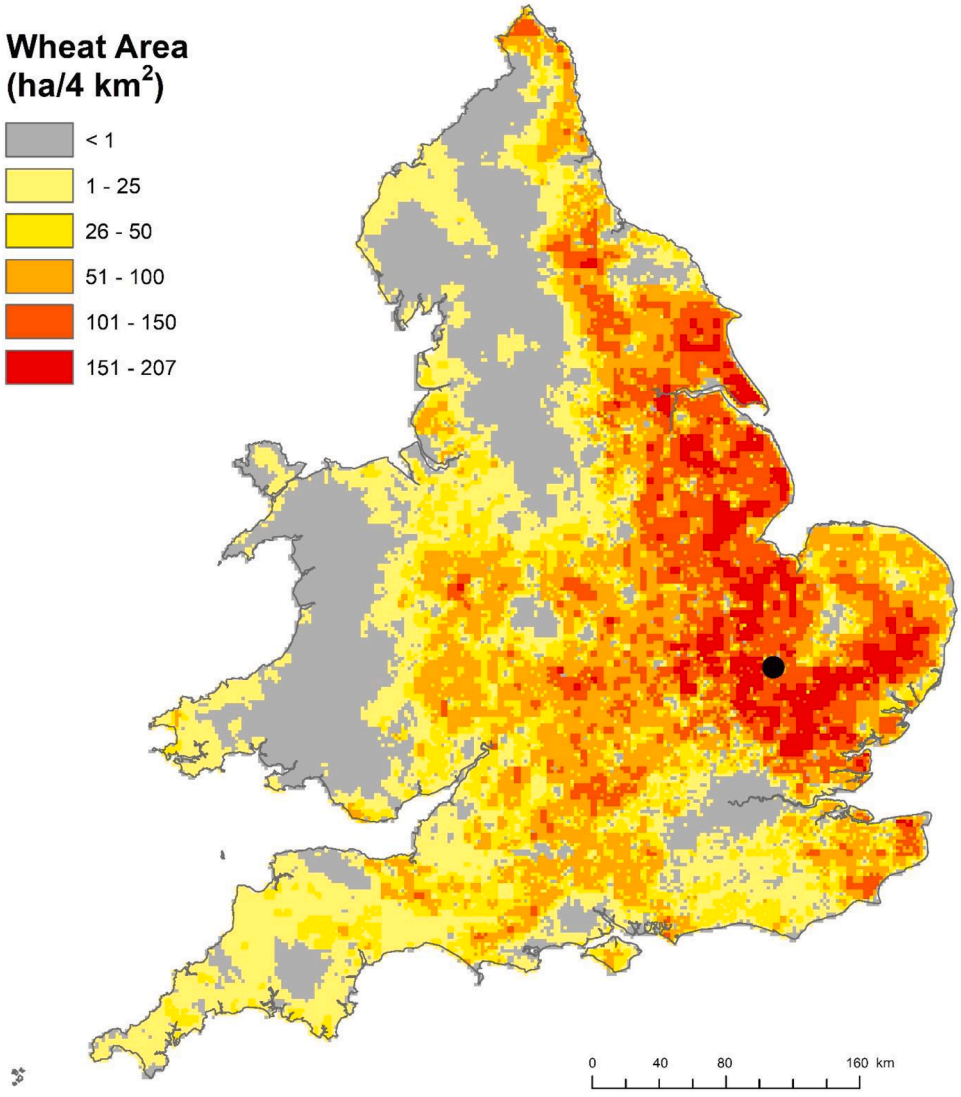

Fig. 2. Reported wheat cropped area (ha per 4 km^2) (EDINA, 2016) and location of study site (Cambridge).

against observed records from recent experimental trials at two sites including Cambridge and St. Neots (which is in very close proximity). Wheat yields for the 105 years weather data were modelled assuming a contemporary variety and high level of agronomic management. Empirical models were developed to predict the simulated wheat yields from the DSIs. Two synthetic future weather datasets were compiled ('near' and 'far' future) and the DSIs that best explained the historical yield variability were used with to estimate future drought-related yield losses. The Sirius model was then run with the synthetic future climatology to estimate future yield losses for comparison against the equivalent DSI-derived values.

2.1. Site characteristics

The study used a representative site at Cambridge in eastern England. Nationally, this is the most important wheat production region, accounting for a quarter (26%) of the UK wheat area and nearly a third (29%) of total production (Defra, 2018) (Fig. 2). It is also the driest region in the UK, receiving an average annual rainfall of 568 mm. The soil was assumed to be a slowly permeable calcareous clayey soil which is typical of arable soils in the region.

2.2. Historical weather dataset

Assessments of historic drought on agriculture require long run climate data to provide stochastic stability and ensure sufficient dry years are included (El Chami et al., 2015). A daily weather dataset was compiled for the Cambridge NIAB Experimental Research Station (Lat: 52°24' N; Lon: 0°10'E; altitude 26 m) for 1912 to 2015 from data collected on site. The adjacent Cambridge Botanical Gardens (Lat: 52°19' N; Lon: 0°13' E) and Met Office Integrated Data Archive System (MIDAS) Land and Marine surface station databank were used for gap filling. If more than a single day of temperature data was missing, the HadCET dataset (Parker et al., 1992) was used for infilling. Solar radiation (MJ m^{-2} d^{-1}) was estimated from daily sunshine hours and daily average vapour pressure (VP) was estimated from the daily minimum temperature (Allen et al., 1998). Daily average wind speed records were only available for 1972 to 2007. As wind speed cannot be readily estimated from other variables, a locally derived average value of 3.5 m s^{-1} was used for years when wind speed was not recorded. Reference evapotranspiration (ETo) was estimated using the Penman-Monteith method (Allen et al., 1998).

2.3. Future synthetic weather datasets

Synthetic daily weather sequences for the site were generated using the LARS-WG stochastic weather generator (Semenov and Barrow, 1997). The LARS-WG can simulate weather data for a given site under both current and future climate conditions. The derived daily time-series include the variables precipitation (mm), maximum and minimum temperature (°C) and solar radiation (MJ $m^{-2}day^{-1}$). The use of LARS-WG to develop climate change scenarios has been described by Semenov and Stratonovitch (2010) and applied extensively to assess crop responses under future climates for various locations (Mavromatis and Hansen, 2001; Semenov and Doblas-Reyes, 2007; Elsgaard et al., 2012; Gohari et al., 2013). The global climate model HadGEM2-ES from the Met Office Hadley Centre for the CMIP5 centennial simulations was used in this study to generate a dataset with a time series of 300 years for three discrete time horizons, termed (i) 'baseline' spanning the period 1981 to 2000, (ii) 'near future' equating to 2031 to 2050, and (iii) 'far future' for 2081 to 2100. A summary of changes in precipitation, temperature and radiation projected by the HadGEM2-ES model for the near and far future time horizons is given in Fig. 3. All future climate scenarios in the 'near' and 'far' periods assumed a high emissions scenario (RCP8.5). The CO_2 concentrations were 369 ppm for 1981-2000, 489 ppm for 2031-2050 and 844 ppm for the 2081-2100 periods, respectively.

The synthetic baseline annual precipitation and reference evapotranspiration (ETo) data were compared with historical data for the site (Fig. 4) for 1975 and 2004, corresponding to years used for comparison with the 'near' and 'far' future scenarios. The synthetic data conserves the median values for precipitation and ETo but contains larger variability (with the generated ETo being less variable than the observed record). A two-sample t-test failed to reject the null hypothesis that the observed and synthetic data were from independent random samples from normal distributions with equal means for both precipitation ($p = 0.612$) and ETo ($p = 0.479$).

2.4. Wheat model parameterisation and validation

The Sirius crop model (Jamieson et al., 1998a) has been used previously to simulate grain yields in a number of agroclimatically contrasting countries including Bulgaria (Ewert et al., 2002), the USA (Jamieson and Semenov, 2000), the UK (Semenov, 2009; 2014) and New Zealand (Senapati et al., 2019). The model simulates biomass

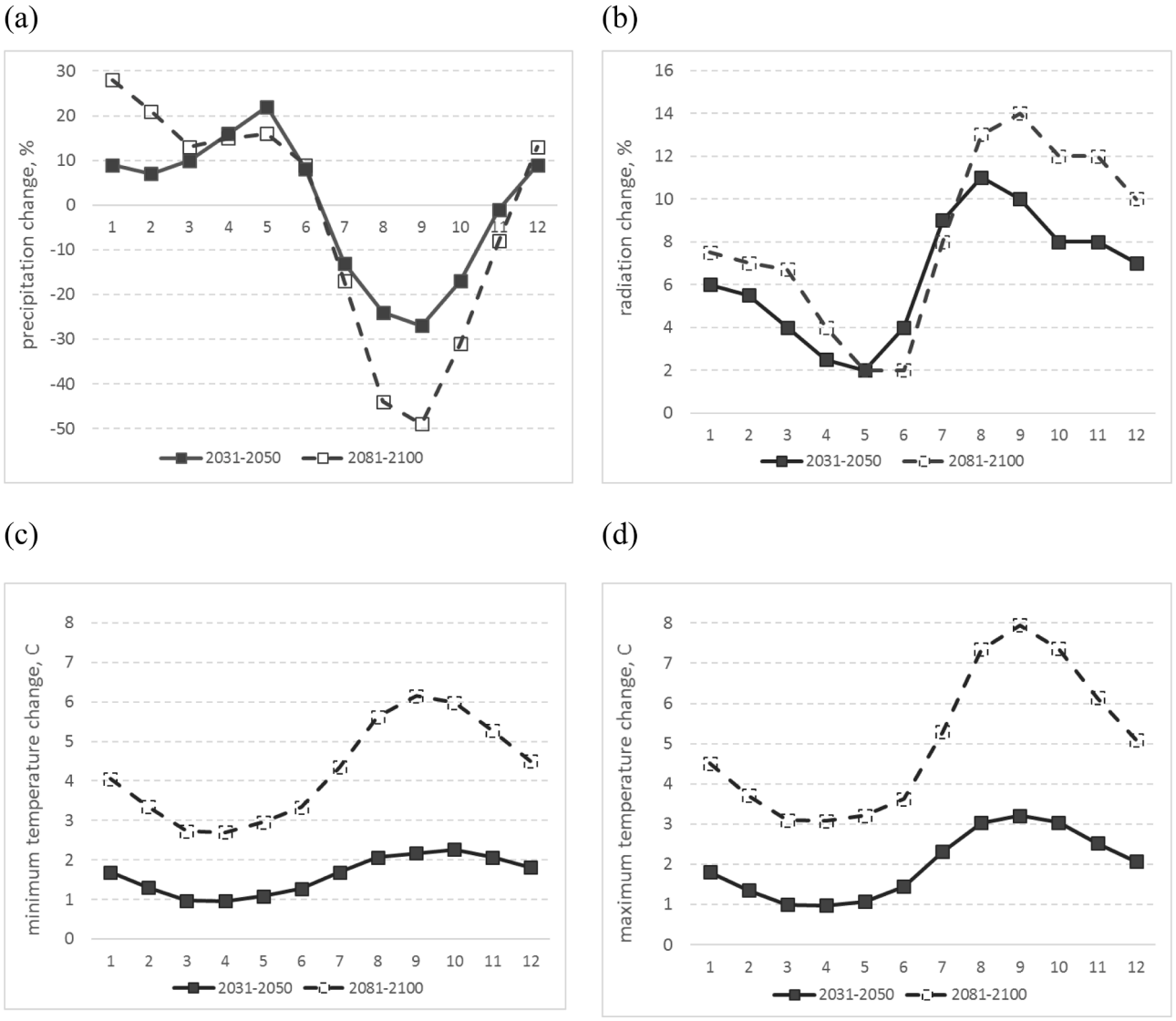

Fig. 3. Changes in monthly precipitation % (a), radiation % (b), minimum (c) and maximum (d) temperature°C as predicted by the HadGEM2-ES climate model from the Met Office Hadley Centre for the RCP8.5 emission scenario for the 'near' (2031-2050) and 'far' (2081-2100) future climate scenarios compared with the baseline (1981-2010) climate.

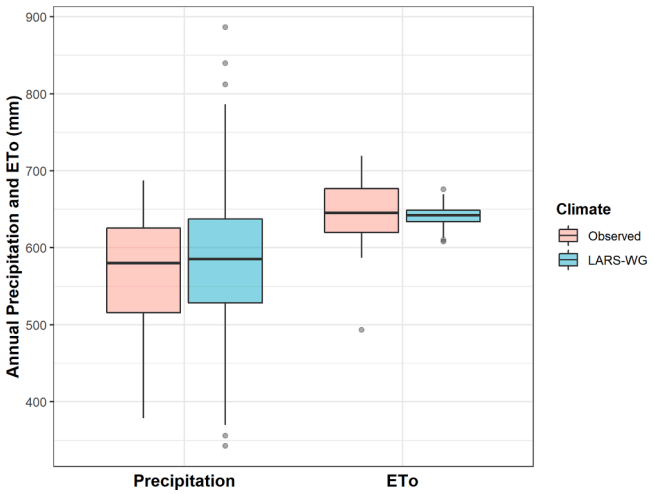

Fig. 4. Boxplots of precipitation (P) and reference evapotranspiration (ETo) for the observed historical data and LARS-WG for the study site at Cambridge.

production from intercepted photosynthetically active radiation and radiation use efficiency. Leaf area index (LAI) is established from a thermal time sub-model, with phenological development being calculated from mainstream leaf appearance rate and final leaf number. Water and nitrogen limitations are simulated through their effects on LAI development and radiation use efficiency. Grain yield is dependent on biomass at anthesis and new biomass is formed after the start of grain filling. In addition, during unstressed conditions, the decline in LAI and end of the grain filling period coincide. However, senescence is accelerated during water-stressed conditions, restricting grain filling and thus reducing final yield (Jamieson et al., 1998b).

The Sirius model has been calibrated for many modern wheat cultivars including cv. Claire used in this study (Semenov et al., 1996; Jamieson et al., 1998; Lawless and Semenov, 2005; Martre et al., 2006; Jamieson et al., 2007; Lawless et al., 2008). The model and calibrated cultivar parameters are available from https://sites.google.com/view/sirius-wheat/. Sirius was extensively tested and validated using available experimental datasets and performed well under diverse climatic conditions across Europe, North and South America, Australia and New Zealand (Asseng et al., 2015; Harkness et al., 2020). Sirius responses to water stress were tested against the rain shelter experiment in Lincoln, New Zealand with 12 treatments varying from no precipitation during the growing season to a fully irrigated treatment (Jamieson et al., 1998c). Responses to increased temperature and CO_2 concentration were validated against the Free-Air CO2 Enrichment (FACE) experiments (Jamieson et al., 2000; Ewert et al., 2002; Asseng et al., 2015) and tested in several global AgMIP studies (Webber at al., 2018; Liu et al., 2019; Asseng et al., 2019).

In the UK, a wide range of wheat cultivars are grown depending on their intended use (e.g., baking, bread making or stock feed), so no single cultivar dominates the market. Each year, the Agriculture and Horticulture Development Board (AHDB), which represents the interests of growers and cereal industry, produces a "recommended list" of varieties, which changes depending on grower and market preferences and varietal development. The only cultivar currently on the AHDB recommended list that has been calibrated in the Sirius model is *cv.* Claire, which is grown on approximately 2% of the total UK wheat area, representing 36,000 hectares. Given the availability of crop development data and parameters relating to emergence, anthesis, maturity and grain protein content, *cv.* Claire was selected for this study (Table 1). The necessary soil parameters for the study site (Evesham 3 soil association) were derived from the LandIS soil series horizon hydraulic dataset (Hollis et al., 2015; NSRI, 2016) with percolation coefficients calculated according to Addiscott and Whitmore (1991) (Table 2).

Table 1
Genetic coefficients used for *cv.* Claire (Source: Rothamsted Research, 2006).

Cultivar parameter	Value
Thermal time from sowing to emergence	150
Thermal time from anthesis to beginning of grain fill	100
Thermal time begging of grain fill to end of grain fill	650
Thermal time end grain fill to harvest maturity	200
Potential maximum leaf size	0.007
Phyllochron in degree days	110
Minimum possible leaf number	8
Absolute maximum leaf number	18
Day length response in leaves per hour of day length	0.5
Response of vernalisation rate to temperature	0.0012
Vernalisation rate (1/days) at 0 C°	0.012
PAR extinction coefficient	0.7
Max protein concentration (% at 15% grain moisture)	15

Table 2
Soil parameters used for the Evesham 3 soil series (NSRI. 2016).

Soil parameter	Value			
Soil depth (m)	0.25	0.5	0.75	1
Saturation moisture content vol% (soil porosity)	55.9	53.6	49.9	48.8
Drained Upper limit vol% at 40 kPa tension	41.4	46.5	43.2	42
Lower limit vol% at 1500 kPa tension (wilting point)	26.6	34.6	32.5	31.7
Percolation coefficient	0.14			
Available water capacity for cereals (mm/m)	120			

A typical sowing date (10th October) for winter wheat was used for each year of simulation. The Sirius model was run assuming no nitrogen limitations and with atmospheric CO_2 levels set to 399 ppm, to correspond to the average value for 2015 (Dlugookencky and Tans, 2016). Thus, the only direct influence on yield in each year related to the weather. Sirius provides outputs for potential (Y_P) yield which is primarily a function of temperature and radiation, and water limited (Y_{WL}) yield (Semenov et al., 2009). In this paper, we define yield loss due to drought as the difference between Y_P and Y_{WL}.

The modelled water limited yields (Y_{WL}) were validated using yield records from 9 AHDB experimental fields at Cambridge (Lat: 52°14' N; Lon: 0°6' E; altitude 20m asl) and St Neots (Lat: 52°15' N; Lon: -0°23' E; 55m asl) which had all cultivated *cv.* Claire over a six year period (1999 to 2005). Model goodness of fit was assessed using the Root Mean Squared Error (RMSE) and Relative RMSE (RRMSE) based on the paired observed and simulated yield data (Loague and Green 1991). Model fit was considered to be 'excellent' if the RRMSE was <10%, 'good' if it was between 10% and 20%, 'fair' if it was greater than 20% and less than 30%, and 'poor' if the values were greater than 30% (Jamieson et al., 1991).

2.5. Drought severity indices (DSI)

Four drought severity indices were considered.

The *Standardized Precipitation Index (SPI)* is based on the probability of precipitation for a given time-scale (Guttman, 1998). A 20 to 30-year precipitation record is fitted to a probability distribution (e.g. gamma or Pearson type III) and then converted into z-scores so that the average SPI for a specified time-step is zero. Deviation from this value provides a classification of either a drought or wet period (Wilhite, 2005; Vicente-Serrano et al., 2012). Complete calculation procedures are available in WMO (2012). The SPI was calculated on a monthly time step from 1912 to 2015 using an open source program (NDMC, n.d) which has been used in previous research (e.g. Pratoomchai et al., 2015).

The *Standardized Precipitation Evapotranspiration Index (SPEI)* is based on the SPI but includes reference evapotranspiration (ETo). A water surplus or deficit for each month is calculated by subtracting ETo from precipitation (Vicente-Serrano et al., 2010). A three-parameter

log-logistic distribution is then used to adjust the calculated surplus or deficit. Values can be accumulated at different time scales (from 1 to 24 months) which are then converted to standard deviations from the average. The SPEI adopts the same drought classification as SPI. The SPEI was calculated on a monthly time step from 1911 to 2015 using the R package SPEI (Beguería and Vicente-Serrano, 2013) which allows users to define parameters that best fit their specific use. In this study, the recommended log-logistic probability distributions, unbiased probability weighted moment distribution functions and default rectangular kernel function were selected.

The *Palmer Drought Severity Index (PDSI)* is based on precipitation, ETo and soil available water capacity (AWC) data for input into a water balance model to assess soil recharge, run off and surface soil moisture loss (Palmer, 1965). The PDSI provides dimensionless values, classified into 11 categories. Monthly values for PDSI from 1911 to 2015 were calculated using a MATLAB tool (Jacobi et al., 2013). Reference evapotranspiration (ETo) was estimated using the Thornthwaite (1948) method.

The *Potential Soil Moisture Deficit (PSMD)* is a useful agroclimatic index that combines the interaction of rainfall and ETo. The variable is calculated from:

$$PSMD_i = PSMD_{i-1} + ET_i - P_i \quad (1)$$

where:

$PSMD_i$ = potential soil moisture deficit at the end of month i, mm

ET_i = potential evapotranspiration in month i, mm

P_i = rainfall in month i, mm

In months where $P_i > (PSMD_{i-1} + ET_i)$, any initial soil moisture deficit is assumed to have been filled and $PSMD_i = 0$. In the UK, soil moisture deficits typically start to accrue in early spring as ET starts to exceed P, peak in mid-summer (July-August) and then decline through autumn and winter as P exceeds ET. The PSMD is always replenished in winter, so estimation of PSMD starts with January as month i = 1 and $PSMD_i = 0$. The maximum value over the 12 months is the $PSMD_{max}$ for that year. The variable is usually computed on a daily time-step. Various studies have shown a strong correlation between irrigation need and the maximum annual value for PSMD (e.g., Rodriguez-Diaz et al., 2007), although no research has previously used this indicator to assess drought risk.

Simulating wheat yield loss due to drought under current and future climate conditions

The relationship between each DSI and simulated yield loss between 1912 and 2015 was assessed using the Spearman's Rank correlation coefficient with a significance threshold of $p < 0.05$, adopting a similar method to that used by Potopová et al. (2015). This was applied to the Sirius modelled yield losses and the four DSIs at various time-steps calculated for each month in each respective growing season. Yield-loss response functions were calibrated for the best fitting time-steps for each DSI, based on the RMSE values. The period 1981-2010 was used to perform the calibration of the response functions. This period coincides with the baseline scenario of the synthetic data. The remaining 80 years were used for validation purposes. The best-fitting DSI response function and the validated Sirius model were then used with each year in the three synthetic weather datasets (baseline, near future and far future) to derive empirical cumulative distribution functions of baseline and future (near and far) yield loss. The rates of change between baseline and future scenario outcomes of the various response functions and the Sirius model then allowed an estimation of the attribution of yield losses to drought under climate change.

3. Results and Discussion

3.1. Yield model validation

Visually, the Sirius simulated yields agree reasonably well with reported yields (Fig. 5) with most observations lying close to the 1:1 line. There was one notable outlier for one field, possibly due to a marked variation in the local soil type and/or discrepancy in the rainfall recorded at St Neots compared to Cambridge. In general, the modelled yields were marginally higher than the observed values. The RMSE varied between 0.55 and 1.6 t ha^{-1}, which corresponds closely with the range of standard deviation (0.7 to 1.1) (Table 3). Overall, the Sirius model performance was considered 'good' as evidenced by the RRMSE values of between 5% and 16% but the simulated wheat yields fitted better for Cambridge (RRMSE 5.48%) compared to the St Neots (11.49%) site.

3.2. Simulated historical yield and drought impacts

The simulated annual yields under 'potential' and 'water limiting' conditions between 1912 and 2015 are shown in Fig. 6. Water limitations prevent crops from attaining their potential yield in most years; however, the average simulated yield loss of 6.1% (equivalent to 0.7 t ha^{-1}) across the time series is not high compared to other studies. For example, El Chami et al. (2015) simulated an average wheat yield loss of 24.6% (1.9 t ha^{-1}) for a site in eastern England using the Aquacrop model, but considered a much shorter time series and for a light textured sandy loam soil, whereas this study used a clay/loamy clay soil with a higher AWC capable of buffering longer periods of low rainfall. The standard deviation of Y_P (0.4 t ha^{-1}) and Y_{WL} (0.9 t ha^{-1}) confirmed that over half (56%) the simulated yield loss was due to water limitations, and 44% was due to variation in other weather-related variables.

Fig. 6 highlights the droughts in 1921, 1934, 1942, 1976, 1996 and 2010 as being the most severe with yield losses ranging from 25-40%. In 2010 wheat yields in eastern England were reported to be 6% below the 5 year average and 11% below the long term record (Defra, 2015). It was also reported that crops were adversely affected by the prolonged dry spell between April and May with continued dry weather during grain

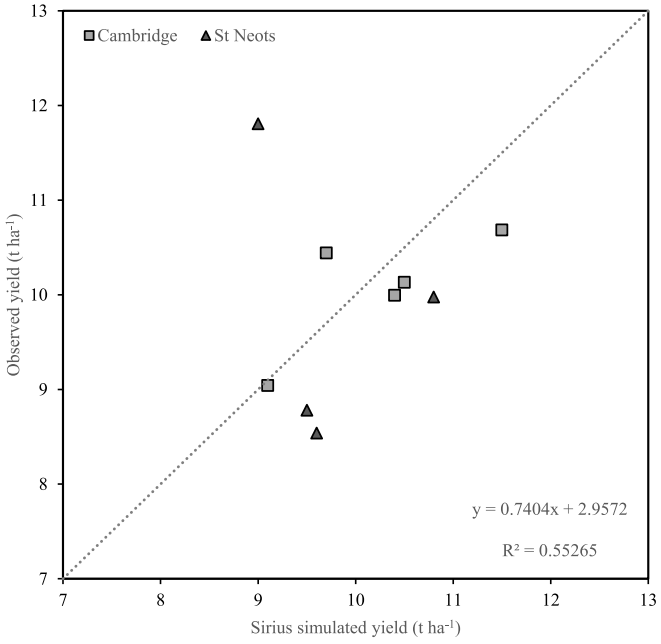

Fig. 5. Comparison between Sirius simulated wheat yield (t ha^{-1}) and observed yield (t ha^{-1}) from AHDB recommended list trials at Cambridge NIAB and St Neots sites.

Table 3
Summary statistics from the Sirius validation for each site, all study sites combined.

Statistic	Field site		
	Cambridge	St Neots	Combined
Number of observations (n)	5	4	9
Mean yield observed (t ha^{-1})	10.06	9.78	9.93
Mean yield simulated (t ha^{-1})	10.24	9.73	10.01
RMSE (t ha^{-1})	0.55	1.6	1.14
RRMSE (%)	5.48	16.34	11.49
Standard Deviation (SD)	0.7	1.1	0.9

filling (June and July) causing drought stress to crops grown on all soil types (Defra, 2010). The extreme yield limiting droughts of 1921, 1976 (Cole and Marsh 2006) and 2010 (Kendon et al., 2013) are well documented. Although the seasonal duration and intensity of the yield limiting droughts differ in the weather record for Cambridge, they all feature dry periods between late May and the middle of July, which correspond to key drought sensitive growth stages for wheat. The 1976 drought in the UK was considered to be one of the most extreme in living memory also affecting most of Central Europe (Spinoni et al. 2015), with reported financial impacts in excess of £500 million due to failed crops and the national average cereal yield being 10 to 15% below the 1970-1974 average (Cole and Marsh, 2006). The drought in 1921 would have led to a yield loss of more than double (38%) that experienced in 1976, however, documented impacts are limited.

3.3. *Correlation of drought indicators with yield loss and response functions*

The relative strength of the correlation between SPI, SPEI and modelled yield losses for different aggregation periods and lags, and the monthly values of PDSI and PSMD are presented as 'heat maps' in Fig. 7. As expected, yield loss correlation with SPI, SPEI and PDSI is negative as higher yield losses occur in drier periods. On the contrary, the correlation with PSMD is positive as higher values of PSMD represent higher

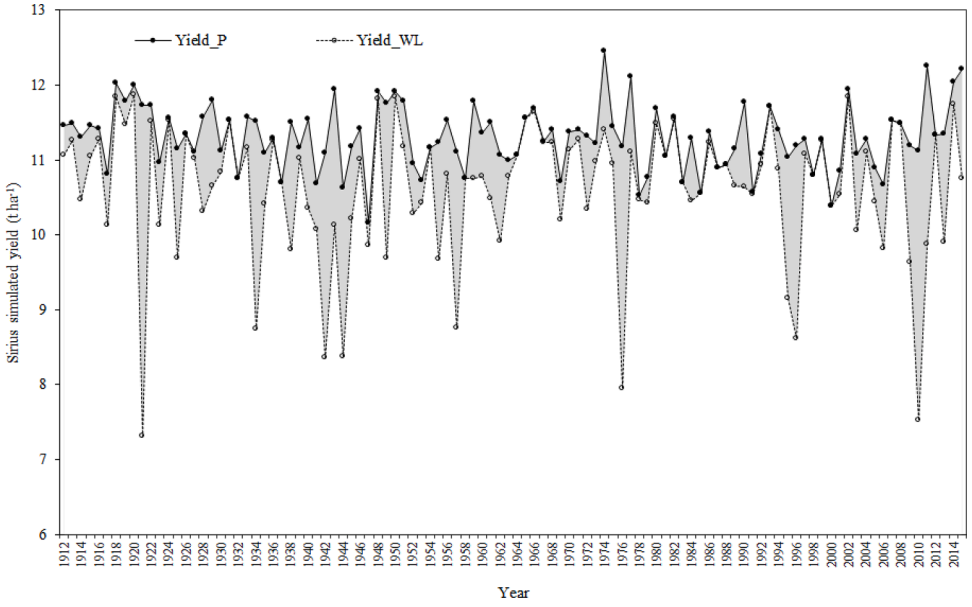

Fig. 6. Sirius simulated annual potential (Yield_P) and water limited (Yield_WL) wheat yield (t ha^{-1}) between 1912 and 2015.

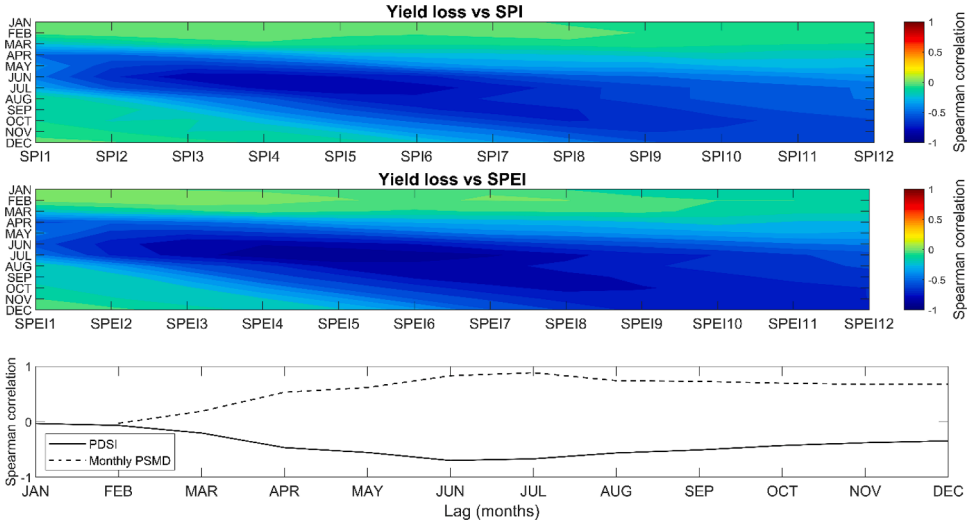

Fig. 7. Heat maps showing the Spearman's Rank correlation coefficient (rho) between monthly SPI and SPEI and Sirius simulated wheat yield loss at Cambridge (1912-2015). Also shown are the monthly correlations between yield and PSMD and PDSI.

aridity and drier conditions. Before April, none of the DSIs show any significant correlation with yield loss, which is consistent with the understanding of water stress impacts during this growth period (El Chami et al., 2015). The correlations then strengthen from April onwards, peaking in June and July, consistent with Dodd et al. (2011) who reported that early stem extension (April), flowering (June) and grain filling (June-July) are particularly drought sensitive stages for wheat.

Potopová et al. (2015b) also showed that the strongest correlation between SPEI and regional winter wheat yield occurred between May and June (anthesis) at 1 to 7 month lags in the Czech Republic. They also found a less pronounced correlation in April (shooting stage). Potopová et al. (2015b) showed how a short-term drought (1 to 2 month) during emergence (October) could influence yield. However, no equivalent correlation was found for the UK, mainly due to the fact that dry autumns tend not to reduce establishment sufficiently enough that compensatory root growth or tillering cannot occur (AHDB, 2015).

The correlations between SPI and SPEI with yield loss do not differ considerably, which is consistent with other humid environments (Paulo et al., 2012; Bachmair et al., 2016), although Vicente-Serrano et al. (2012) reported that SPEI shows the strongest correlation to wheat yield. Due to its simplicity, SPI may be more suited than SPEI for UK drought monitoring for wheat. However, under a changing climate, evapotranspiration rates are expected to increase (Richter and Semenov, 2005; Daccache et al., 2011) meaning that the SPEI may become more suited for use in the UK in the future (Haro-Monteagudo et al., 2017).

Despite the potential for using the PDSI to identify yield-limiting droughts earlier in the season, it fails to maintain its relative advantage over other DSIs during the more sensitive growth stages. Its strongest correlation, June (-0.70) was weaker than the strongest correlation of other indicators (SPI-5_{Jul}=-0.80; SPEI-5_{Jul}=-0.89; $PSMD_{Jul}$=0.88). This is consistent with previous research that showed that multi-scalar indices such as SPI and SPEI generally outperform indices with fixed time steps such as PDSI in identifying agricultural impacts (Paulo et al., 2012; Vicente-Serrano et al., 2012), although some studies have found PDSI to be better linked to agricultural impacts (Tunaloglu and Durdu, 2012).

3.4. Yield loss – DSI response functions

Fig. 8 shows the estimated yield loss against the highest correlated variant for each DSI, i.e. SPI-5_{Jul}, SPEI-5_{Jul}, $PDSI_{Jun}$ and $PSMD_{Jul}$. In all four cases, the distribution and shape of the cloud of points suggests a non-linear relationship. An exponential fit was used due to the yield losses asymptotically approach zero as DSI increases (SPI, SPEI and PDSI) or decreases (PSMD).The fitted exponential response function corresponding to SPEI-5_{Jul} performs better than the other three indicators with regards to RMSE and also in terms of the explained variance (r^2) followed by $PSMD_{July}$. The corresponding response function is

$$YL_t = 0.3141 \cdot e^{-1.23 \cdot SPEI-5_{Jul\,t}}$$

where YL_t represents the yield loss in year t and $SPEI-5_{Jult}$ is the corresponding DSI value in year t.

From Fig. 8 it is also possible to observe the sensitivity of wheat to weather variability and the need for moist conditions throughout the growing season to achieve maximum yield, or at least not to suffer significant yield losses. For SPI, SPEI and PDSI, the yield losses start to accrue under conditions that would be considered wet (below 1.0 for SPI and SPEI, and below 2.0 for PDSI). The same applies to PSMD, although this is not as evident as it is not a standardised indicator. The median observed PSMD value was 171 mm with yield losses starting from values around 100 mm.

3.5. Future wheat yield losses

Fig. 9 shows the cumulative distribution functions calculated for the resulting 300 yield loss values from each scenario (baseline, near and far future) as a function of SPEI-5_{July} (Fig. 9a) and with the equivalent outputs from the Sirius wheat modelling (Fig. 9b). The results obtained using the response function for SPEI-5_{July} (Fig. 9a) show that under the baseline scenario (blue dots), yield losses are predicted to be 0.25 t ha^{-1} on average (50% probability of exceedance). In dry years (≤20% probability of exceedance), the yield losses might exceed 0.7 t ha^{-1}. The 'near' future scenario (red dots) is predicted to result in a significantly worse situation compared to the baseline, with yield losses ranging from 0.9 t ha^{-1} on average and 2.0 t ha^{-1} in dry years, representing a three to

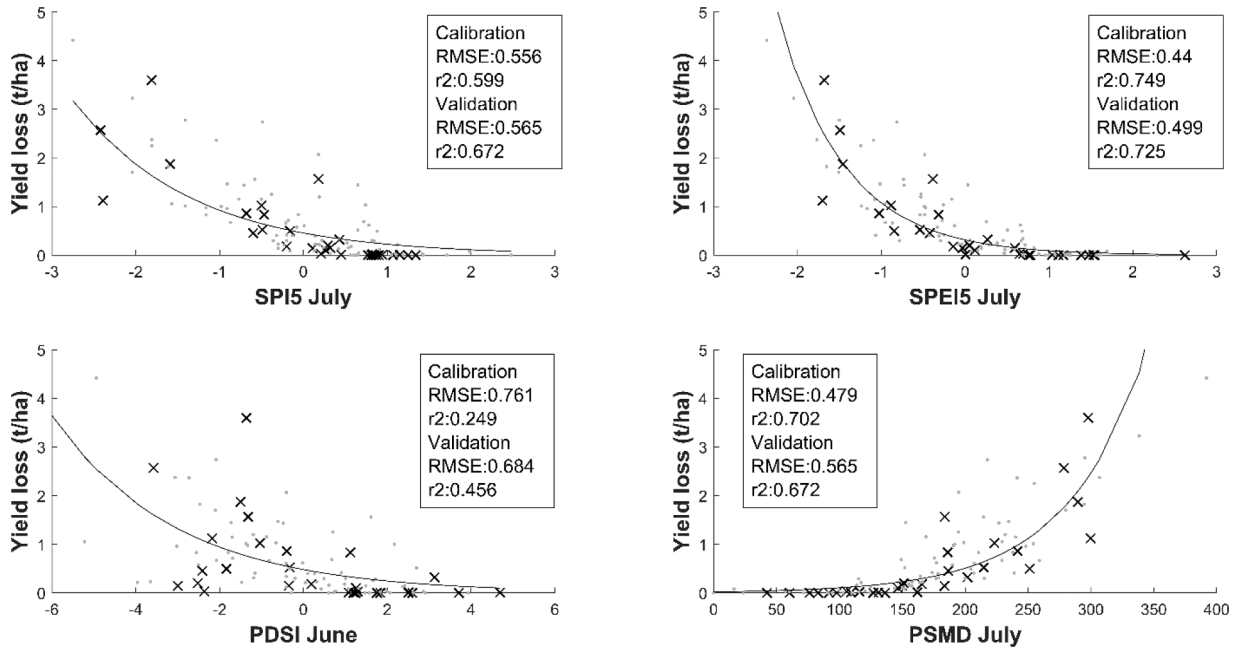

Fig. 8. Calculated wheat annual yield loss against the highest correlated accumulation and time step for all four tested DSIs and fitted exponential response functions with goodness-of-fit indicators RMSE and r2 for calibration (×) and validation (grey circles).

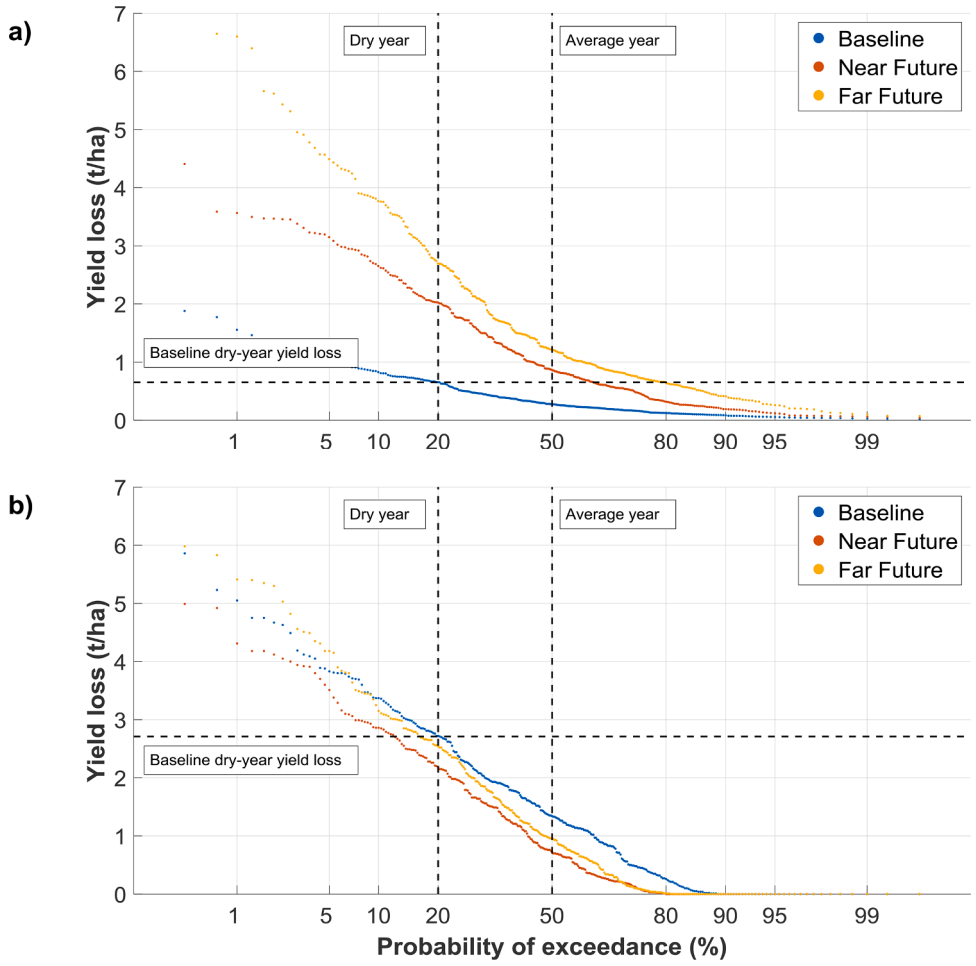

Fig. 9. Cumulative distribution functions of yield loss calculated as a function of SPEI-5_{July} (a) and with Sirius wheat model (b) for the baseline, near future, and far future climate scenarios from LARS-WG.

three and a half fold increase in losses from the baseline. The consequences of weather in the 'far' future scenario (yellow dots) on yield losses are even higher, with yield losses expected to occur in most years, with average and dry year losses equivalent to 1.25 t ha^{-1} and 2.8 t ha^{-1}, respectively. This represents a four to fivefold increase with reference to the baseline. Therefore, whilst the 'near' future scenario does show a significant worsening of current conditions, if the current trajectory of climate evolves towards a 'far' future scenario, then approximately 80% of future years based on the DSI approach would experience conditions that are currently considered by growers to be a 'dry' year. This would have serious implications for rainfed production particularly for farming businesses in the drier eastern regions growing cereals on low moisture retentive soils. Drought adaptation responses would need to include evaluating the economic viability of supplemental irrigation, switching to more drought tolerant varieties and modifying cropping calendars.

In contrast, the results from the Sirius modelling (Fig. 9b) shows that under the baseline scenario (blue dots), yield losses are predicted to be significantly higher – around 1.4 t ha^{-1} on average and exceeding 2.7 t ha^{-1} in dry years. The 'near' future scenario (red dots) shows both a reduction in the frequency of losses and their magnitude (0.7 t ha^{-1} on average and 2.2 t ha^{-1} in dry years). Under the 'far' future scenario (yellow dots), the intensity of yield losses during dry years is close to the baseline level (2.6 t ha^{-1}) but under average conditions (1.0 t ha^{-1}) is only marginally higher than the 'near' future scenario.

The two contrasting approaches to assess current and future drought risks on wheat yield result in very different absolute values and trends over time, which have important repercussions when considering how best to support the cereal industry in drought management planning. For the baseline situation, the comparison shows that the use of the response function for SPEI-5_{July} tends to over-estimate yield losses in wet years and under-estimate losses in dry years, when compared against the ecophysiological modelling approach. In addition, the projected increases in monthly water deficits under the future scenarios means that the use of SPEI-5_{July} results in higher yield losses, but excludes other important aspects, including, for example, the positive impacts associated with rising CO_2 concentration levels on crop growth and advances in phenological development resulting in avoidance of severe drought. There is of course extensive literature on the impacts of rising CO_2 concentrations on crop growth. For example, simulation runs using the Sirius model with a constant baseline CO_2 concentration for the present and future 2050 climates, and with elevated CO_2 concentrations for the future 2050s climate across Europe has previously been undertaken. Readers interested in that work are referred to Semenov and Shewry (2011). When comparing different approaches (DSI response function and Sirius) it is also important to consider the 'relative' rates of change. The under-estimation of ETo variability in the synthetic weather dataset from the LARS-WG (Fig. 4) coupled with the choice of curve fitting statistic (quadratic or exponential) used to derive the response functions (Fig. 8) could also be important contributory factors that explain the large absolute differences between the two yield loss prediction approaches.

The Sirius model simulations showed that the onset of the anthesis period and the date of maturity will occur earlier (8 and 11 days for the 'near' future scenario, and 17 and 23 days, for the 'far' future scenario,

respectively). This means that despite the high correlation observed between SPEI-5_{July} and yield losses for the current (baseline) climate, this correlation will not necessarily be valid under a future climate, due to a shift in the cropping calendar. The use of DSIs for future drought related yield loss assessments would therefore need to consider other accumulation periods and months to correspond with changing crop calendars. These results provide valuable new insights to complement previous research on climate impacts on wheat. For example, Semenov (2008) showed that average yields were projected to increase and the impact of drought stress on UK wheat production might actually decrease under a changing climate. That study concluded that the frequency of heat stress days around flowering might be a more serious problem for sustainable wheat production under a changing climate. The modelling in this study confirmed that predicted future average yield losses would be moderated by the more favourable higher temperatures for crop growth, but in very dry years extreme high temperatures would impact on crop development and final yield.

3.6. Methodological limitations

Accessing reliable, long-term and complete historical weather time series is always a challenge for agricultural research. Whilst long-term records for temperature and precipitation were available, values for other variables including wind speed, vapour pressure and solar radiation were incomplete and had to be estimated. Reasonably high resolution gridded long-term (100 year) weather datasets for the 20th Century (CEH-GEAR) (Keller et al. 2015) and detailed national soils information were available (Hollis et al., 2015) but there remains limited cultivar specific information relating to crop development and yields for crop modelling. Although detailed experimental field records were available to support Sirius model validation for *cv.* Claire, there was limited data to calibrate and validate more recent cultivars, particularly regarding dates for the timing of key growth stages. Although simulation runs using the Sirius model with a constant baseline CO_2 concentration for the present and future (2050s) climates, and with elevated CO_2 concentrations for the future climate across Europe have been conducted (Semenov and Shewry, 2011), one of the limitations of the DSI approach described here is that it ignores the beneficial effects of elevated CO_2. Further work could thus quantify this by conducting additional Sirius model runs for the future time series maintaining atmospheric CO_2 at current levels. The difference in drought induced yield losses between the existing DSI simulations (as reported here) and the new outputs would help quantify how much elevated CO_2 levels might reduce drought related stress and the associated yield losses for this case study site.

Finally, the spatial scale was limited to a single site (Cambridge); although this is considered representative of an area that has a significant proportion of the national wheat cropped area, it would be useful to extend the analyses to other important production regions, including central England and the east coast, and across a wider range of soil types. Indeed, the importance of spatial scale and soil heterogeneity was also highlighted by Harkness et al (2020) who also assumed a single soil for their Sirius modelling, but noted that soil depth and type, as well as other landscape characteristics strongly influence both the frequency and severity of adverse weather impacts, including short-term drought and prolonged water stress.

3.7. Implications

Most arable (cereal) production in the UK is rainfed and following a spate of relatively 'wet' years, it is not surprising that many farmers have not considered the economic risks associated with rainfall deficits on crop yields. However, the drought in 2018 and heatwave in 2019 highlighted the water-related risks to both rainfed and irrigated production with consequences for farmers, grain merchants, processors and retailers (Knox and Hess, 2019). Whilst most farmers are well attuned to managing short-term weather-related crop risks, they still lack access to tools to support medium-term decision-making and risk management strategies under conditions of increasing water scarcity and climate uncertainty (Haro-Monteagudo et al., 2019.). Other factors are also important including the scale of the businesses, cropping patterns and whether supplemental irrigation is available to mitigate drought risk. There is thus a need to consider how drought severity indicators, such as those considered here, as well as outputs from crop modelling might be usefully incorporated into farm-scale decision-making to improve drought risk management. In England the water regulatory authority (Environment Agency) monitors the onset of drought using hydro-hydrological thresholds and environmental indicators (EA, 2015). Whilst the economic impacts of agricultural drought are recognised (Rey et al., 2017), tools and approaches to understand and manage agronomic impacts are still absent. The approaches described here could be used in support of developing new tools for farmers and the agri-food industry to better understand the impacts of drought on productivity and the adaptation options available to minimise drought impacts. However, this study confirms that whilst drought severity indicators can be useful for assessing meteorological (rainfall deficit) or agricultural (soil moisture) impacts, their utility for quantifying impacts on crop productivity should be used with caution, particularly when considering future drought risks. Drought indicators remain useful for assessing the severity of particular dry spells for comparison against other events, but since crop productivity depends on other variables not reflected in the response functions, similar drought events can have completely different agronomic outcomes.

4. Conclusions

Water limitations on average reduce UK wheat yields by 1 to 2 t ha^{-1} although this can be considerably higher in drought years. With the frequency and intensity of droughts projected to increase, an improved understanding of likely impacts and farmer adaptation responses are required. By combining the outputs from the Sirius crop model with data from four drought severity indicators, a comparative assessment of the impacts of drought risk on yield losses have been evaluated, for current (baseline) and two future (2031 to 2050, and 2081 to 2100) climate conditions.

For the baseline, all DSIs showed significant correlations on monthly time-steps between April and August, with SPI, SPEI and PSMD showing the strongest correlation for periods that incorporated the end of the 'construction' phase and entire 'production' phase for wheat development. Comparative analysis between the two approaches (DSI and Sirius modelling) highlighted large differences in estimated yield loss attributed to drought, both in terms of direction and magnitude, for both the baseline and future scenario. For the DSI approach, future yield losses increased (up to 1.25 t ha^{-1} and 2.8 t ha^{-1}, for average and dry years, respectively). In contrast, the Sirius modelling showed a slight reduction in future average yield loss (down from a baseline 1.4 t ha^{-1} to 1.0 t ha^{-1}) but negligible change for a future dry year (baseline 2.7 t ha^{-1} to 'far' future 2.6 t ha^{-1}).

The study has highlighted the risks in adopting solely a DSI response function-based approach, particularly in estimating future drought yield losses, where autonomous adaptation including changes in crop calendars coupled with the impacts of CO_2 fertilisation effects on crop yield are not incorporated. A more robust approach therefore lies in integrating hydro-meteorological knowledge from DSIs to quantify the onset, extent and severity of specific drought events coupled with biophysical modelling to assess crop yield responses to limited soil moisture availability in order to inform selection of appropriate responses that minimise the agronomic and economic impacts of drought.

Declaration of competing Interest

The authors declare that they have no known competing financial

interests or personal relationships that could have appeared to influence the work reported in this paper.

Acknowledgement

The authors acknowledge the Class Stiftung Foundation their financial support, Cambridge NIAB for solar radiation data, Cranfield Soil and Agrifood Institute for the soil characteristics data, AHDB for access to their Recommended List Trial yield data. We are grateful for access to the UK Meteorological Office MIDAS Land Surface Stations data (1853-current) from the British Atmospheric Data Centre (http://badc.nerc.ac.uk/data/ukmo-midas). Rothamsted Research receives grant-aided support from the Biotechnology and Biological Sciences Research Council through Designing Future Wheat [BB/P016855/1] and Achieving Sustainable Agricultural Systems [NE/N018125/1].

References

Addiscott, T.M., Whitmore, A.P., 1991. Simulation of solute leaching in soils of differing permeabilities. Soil Use and Management 7 (2), 94–102.

AHDB. 2015. Wheat growth guide. Available at https://cereals.ahdb.org.uk/crop-management/growth-guides.aspx.

Allen, R.G., Pereira, L.S., Raes, D., Smith., M., 1998. Crop evapotranspiration: Guidelines for computing crop requirements. Irrigation and Drainage Paper No 56, FAO.

Asseng, S., Ewert, F., Martre, P., Rotter, R.P., Lobell, D.B., Cammarano, D., Kimball, B.A., Ottman, M.J., Wall, G.W., White, J.W., Reynolds, M.P., Alderman, P.D., Prasad, P.V. V., Aggarwal, P.K., Anothai, J., Basso, B., Biernath, C., Challinor, A.J., De Sanctis, G., Doltra, J., Fereres, E., Garcia-Vile, M., Gayler, S., Hoogenboom, G., Hunt, L.A., Izaurralde, R.C., Jabloun, M., Jones, C.D., Kersebaum, K.C., Koehler, A.K., Muller, C., Kumar, S.N., Nendel, C., O'Leary, G., Olesen, J.E., Palosuo, T., Priesack, E., Rezaei, E. E., Ruane, A.C., Semenov, M.A., Shcherbak, I., Stockle, C., Stratonovitch, P., Streck, T., Supit, I., Tao, F., Thorburn, P.J., Waha, K., Wang, E., Wallach, D., Wolf, I., Zhao, Z., Zhu, Y., 2015. Rising temperatures reduce global wheat production. Nature Climate Change 5, 143–147.

Asseng, S., Martre, P., Maiorano, A., Rotter, R.P., O'Leary, G.J., Fitzgerald, G.J., Girousse, C., Motzo, R., Giunta, F., Babar, M.A., Reynolds, M.P., Kheir, A.M.S., Thorburn, P.J., Waha, K., Ruane, A.C., Aggarwal, P.K., Ahmed, M., Balkovic, J., Basso, B., Biernath, C., Bindi, M., Cammarano, D., Challinor, A.J., De Sanctis, G., Dumont, B., Rezaei, E.E., Fereres, E., Ferrise, R., Garcia-Vila, M., Gayler, S., Gao, Y. J., Horan, H., Hoogenboom, G., Izaurralde, R.C., Jabloun, M., Jones, C.D., Kassie, B. T., Kersebaum, K.C., Klein, C., Koehler, A.K., Liu, B., Minoli, S., San Martin, M.M., Muller, C., Kumar, S.N., Nendel, C., Olesen, J.E., Palosuo, T., Porter, J.R., Priesack, E., Ripoche, D., Semenov, M.A., Stockle, C., Stratonovitch, P., Streck, T., Supit, I., Tao, F.L., Van der Velde, M., Wallach, D., Wang, E.L., Webber, H., Wolf, J., Xiao, L.J., Zhang, Z., Zhao, Z.G., Zhu, Y., Ewert, F., 2019. Climate change impact and adaptation for wheat protein. Global Change Biology 25, 155–173.

Bachmair, S., Svensson, C., Hannaford, J., Barker, L.J., Stahl, K., 2016. A quantitative analysis to objectively appraise drought indicators and model drought impacts. Hydrology and Earth System Sciences 20 (7), 2589.

Baker, F.W., 1989. Drought Resistance in Cereals. CAB International, Exeter.

Beguería, S., Vicente-Serrano, S.M., 2013. SPEI: calculation of the standardised precipitation-evapotranspiration index. R package version, 1.

Burke, E.J., Brown, S.J., 2010. Regional drought over the UK and changes in the future. Journal of Hydrology 394 (3), 471–485.

Burke, E.J., Perry, R.H., Brown, S.J., 2010. An extreme value analysis of UK drought and projections of change in the future. Journal of Hydrology 388 (1), 131–143.

El Chami, D., Knox, J.W., Daccache, A., Weatherhead, E.K., 2015. The economics of irrigating wheat in a humid climate - A study in the East of England. Agricultural Systems 133, 97–108.

Cole, G, Marsh, T, 2006. The impact of climate change on severe droughts. Major drought. England and Wales from 1800 and evidence of impact. Science Report for the Environment Agency –SC040068/SR1.

Daccache, A., Weatherhead, E.K., Stalham, M.A., Knox, J.W, 2011. Impacts of climate change on irrigated potato production in a humid climate. Agricultural and Forest Meteorology 151, 1641–1653.

Defra. 2010. Agriculture in the United Kingdom 2010. 22.

Defra, 2018. Agriculture in the United Kingdom. Natl. Stat. 1–107.

Dlugookencky, E., and Tans, P., 2016. Globally averaged marine surface annual mean data. NOAA/ESRL; https://www.esrl.noaa.gov/gmd/ccgg/trends/global.html.

Dodd, I.C., Whalley, W.R., Ober, E.S., Parry, M.A.J., 2011. Genetic and management approaches to boost UK wheat yields by ameliorating water deficits. Journal of Experimental Botany 62 (15), 5241–5248.

Elsgaard, L., Børgesen, C.D., Olesen, J.E., Siebert, S., Ewert, F., Peltonen-Sainio, P., Skjelvåg, A.O., 2012. Shifts in comparative advantages for maize, oat and wheat cropping under climate change in Europe. Food Additives & Contaminants: Part A 29 (10), 1514–1526.

Ewert, F., Rodriguez, D., Jamieson, P., Semenov, M.A., Mitchell, R.A.C., Goudriaan, J., Porter, J.R., Kimball, B.A., Pinter, P.J., Manderscheid, R., Weigel, H.J., 2002. Effects of elevated CO_2 and drought on wheat: testing crop simulation models for different experimental and climatic conditions. Agriculture Ecosystems and Environment 93, 249–266.

Ewert, F., Rötter, R.P., Bindi, M., Webber, H., Trnka, M., Kersebaum, K.C., Olesen, J.E., van Ittersum, M.K., Janssen, S., Rivington, M., Semenov, M.A., Wallach, D., Porter, J. R., Stewart, D., Verhagen, J., Gaiser, T., Palosuo, T., Tao, F., Nendel, C., Roggero, P. P., Bartošová, L., Asseng, S., 2015. Crop modelling for integrated assessment of risk to food production from climate change. Environmental Modelling & Software 72, 287–303.

FAO, 2017. Sustainable crop production intensification, policy support and governance, food and agriculture organization of the United Nations (http://www.fao.org/3/a-i7477e.pdfen/) Accessed 12.08.2020.

FAOSTAT 2017 http://www.fao.org/faostat/en/#data/QC. Accessed March 2018.

Glotter, M., Elliott, J., 2016. Simulating US agriculture in a modern Dust Bowl drought. Nature Plants 3 (1), 1–6.

Gohari, A., Eslamian, S., Abedi-Koupaei, J., Bavani, A.M., Wang, D., Madani, K., 2013. Climate change impacts on crop production in Iran's Zayandeh-Rud River Basin. Science of the Total Environment 442, 405–419.

Guttman, N.B., 1998. Comparing the Palmer drought index and the standardized precipitation index. Journal of American Water Resources 34 (1), 113–121.

Hall, A.J., Richards, R.A., 2013. Prognosis for genetic improvement of yield potential and water-limited yield of major grain crops. Field Crops Research 143, 18–33.

Harkness, C., Semenov, M.A., Areal, F., Senapati, N., Trnka, M., Balek, J., Bishop, J., 2020. Adverse weather conditions for UK wheat production under climate change. Agricultural and Forest Meteorology 282-283, 107862.

Haro-Monteagudo, D., Daccache, A., Knox, J.W., 2017. Exploring the utility of drought and water scarcity indicators to assess climate risks to agricultural productivity in a humid climate. Hydrology Research. https://doi.org/10.2166/nh.2017.010.

Haro-Monteagudo, D., Knox, J.W., Holman, I.P., 2019. D-Risk: a decision-support webtool for improving drought risk management in irrigated agriculture. Computers and Electronics in Agriculture 162, 855–858.

Hollis, J.M., Lilly, A., Higgins, A., Jones, R.J.A., Keay, C.A., Bellamy, P., 2015. Predicting the water retention characteristics of UK mineral soils. European Journal of Soil Science 66 (1), 239–252.

Ilbery, B., Maye, D., Ingram, J., Little, R., 2013. Risk perception, crop protection and plant disease in the UK wheat sector. Geoforum 50, 129–137.

Jacobi, J., Perrone, D., Duncan, L.L., Hornberger, G., 2013. A tool for calculating the palmer drought indices. Water Resources Research 49, 6086–6089.

Jamieson, P.D., Semenov, M.A., Brooking, I.R., Francis, G.S., 1998a. Sirius: a mechanistic model of wheat response to environmental variation. Eur Journal Agronomy 8, 161–179.

Jamieson, P.D., Porter, J.R., Goudriaan, J., Ritchie, J.V., Van Keulen, H., Stol, W., 1998b. A comparison of the models AFRCWHEAT2, CERES-Wheat, Sirius, SUCROS2 and SWHEAT with measurements from wheat grown under drought. Field Crops Research 55, 23–44.

Jamieson, P.D., Brooking, I.R., Semenov, M.A., Porter, J.R., 1998c. Making sense of wheat development: a critique of methodology. Field Crops Research 55, 117–127.

Jamieson, P.D., Porter, J.R., Wilson, D.R., 1991. A test of the computer simulation model ARCWHEAT1 on wheat crops grown in New Zealand. Field Crops Research 27, 337–350.

Jamieson, P.D., Semenov, M.A., 2000. Modelling nitrogen uptake and redistribution in wheat. Field Crops Research 68 (1), 21–29.

Jamieson, P.D., Berntsen, J., Ewert, F., Kimball, B.A., Olesen, J.E., Pinter, P.J.J., Porter, J.R., Semenov, M.A., 2000. Modelling CO_2 effects on wheat with varying nitrogen supplies. Agriculture, Ecosystems and Environment 82, 27–37.

Jamieson, P.D., Brooking, I.R., Semenov, M.A., MeMaster, G.S., White, J.W., Porter, J.R., 2007. Reconciling alternative models of phenological development in winter wheat. Field Crops Research 103, 36–41.

Kahiluoto, H., Kaseva, J., Balek, J., Olesen, J.E., Ruiz-Ramos, M., Gobin, A., Kersebaum, K.C., Takáč, J., Ruget, F., Ferrise, R., Bezak, P., 2019. Decline in climate resilience of European wheat. Proceedings of the National Academy of Sciences 116 (1), 123–128.

Keller, V.D.J., Tanguy, M., Prosdocimi, I., Terry, J.A., Hitt, O., Cole, S.J., Fry, M., Morris, D.G., Dixon, H., 2015. CEH-GEAR: 1 km resolution daily and monthly areal rainfall estimates for the UK for hydrological and other applications. Earth System Science Data 7 (1), 143–155.

Kendon, M., Marsh, T., Parry, S., 2013. The 2010-2012 drought in England and Wales. Weather 68, 88–95.

Knox, J.W., Haro-Monteagudo, D., Hess, T.M., Morris, J., 2018. Identifying trade-offs and reconciling competing demands for water: Integrating agriculture into a robust decision-making framework. Earth's Future 6 (10), 1457–1470.

Knox, J.W., Hess, T.M., 2019. High level review of the Optimum Water Use methodology for agriculture following the 2018 drought in England. Technical Briefing Note for EA.

Lawless, C., Semenov, M.A., 2005. Assessing lead-time for predicting wheat growth using a crop simulation model. Agricultural and Forest Meteorology 135, 302–313.

Lawless, C., Semenov, M.A., Jamieson, P.D., 2008. Quantifying the effect of uncertainty in soil moisture characteristics on plant growth using a crop simulation model. Field Crops Research 106, 138–147.

Loague, K., Green, R.E., 1991. Statistical and graphical methods for evaluating solute transport models: Overview and application. Journal of Contaminated Hydrology 7, 51–73.

Marsh, T., Cole, G., Wilby, R., 2007. Major droughts in England and Wales, 1800–2006. Weather 62, 87–93.

Martre, P., Jamieson, P.D., Semenov, M.A., Zyskowski, R.F., Porter, J.R., Triboi, E., 2006. Modelling protein content and composition in relation to crop nitrogen dynamics for wheat. European Journal of Agronomy 25, 138–154.

Mavromatis, T., Hansen, J.W., 2001. Inter annual variability characteristics and simulated crop response of four stochastic weather generators. Agricultural and Forest Meteorology 109 (4), 283–296.
NSRI. 2016. Soil Series Horizon Properties, HORIZON Fundamentals, Soil Series Horizon Summary Data. National Soil Resource Institute. Available at http://www.landis.org.uk/data/horhydraulics.cfm (accessed 26 July 2016).
Ober, E.S., Werner, P., Flatman, E., Angus, B., Jack, P., Tapsell, C. 2011. Improving water use efficiency and drought tolerance in UK winter wheats (Project Report 476).
Palmer, 1965. Meteorological drought. Vol 30. Washington. USA: US Department of Commerce, Weather Bureau, DC.
Parker, D.E., Legg, T.P., Folland, C.K., 1992. A new daily Central England Temperature series, 1772–1991. International Journal of Climatology 12, 317–342.
Paulo, A.A., Rosa, R.D., Pereira, L.S., 2012. Climate trends and behaviour of drought indices based on precipitation and evapotranspiration in Portugal. Natural Hazards Earth System Science 12, 1481–1491.
Potopová, V., Štěpánek, P., Možný, M., Soukup, J., 2015. Performance of the standardised precipitation evapotranspiration index at various lags for agricultural drought risk assessment in the Czech Republic. Agricultural and Forest Meteorology 202, 26–38.
Pratoomchai, W., Kazama, S., Manandhar, S., Ekkawatpanit, C., Saphaokham, S., Komori, D., Thongduang, J., 2015. Sharing of people's perceptions of past and future hydro-meteorological changes in the groundwater use area. Water Res Manage 29 (10), 3807–3821.
Rahiz, M., New, M., 2013. 21st century drought scenarios for the UK. Water Resources Management 27 (4), 1039–1061.
Rey, D., Holman, I.P., Knox, J.W., 2017. Developing drought resilience in irrigated agriculture in the face of increasing water scarcity. Reg Environ Change 17 (5), 1527–1540.
Reynolds, M., et al., 2009. Raising yield potential in wheat. J.Exp. Bot. 60, 1899–1918.
Richter, G.M., Semenov, M.A., 2005. Modelling impacts of climate change on wheat yields in England and Wales: Assessing drought risks. Agricultural Systems 84, 77–97.
Rodriguez-Diaz, J.R., Weatherhead, E.K., Knox, J.W., Camacho, E., 2007. Climate change impacts on irrigation water requirements in the Guadalquivir river basin in Spain. Regional Environmental Change 7 (3), 149–159.
Rothamsted Research. 2006. Sirius download. http://resources.rothamsted.ac.uk/mas-models/sirius.
Semenov, M.A., Wolf, J., Evans, L.G., Eckersten, H., Iglesias, A., 1996. Comparison of wheat simulation models under climate change .2. Application of climate change scenarios. Climate Research 7, 271–281.
Semenov, M.A., Barrow, E.M., 1997. Use of a stochastic weather generator in the development of climate change scenarios. Climatic Change 35 (4), 397–414.
Semenov, M.A., Doblas-Reyes, F.J., 2007. Utility of dynamical seasonal forecasts in predicting crop yield. Climate Research 34 (1), 71–81.
Semenov, M.A., 2008. Impacts of climate change on wheat in England and Wales. J. R. Soc. Interface 6 (33), 343–350.
Semenov, M.A., Martre, P., Jamieson, P.D., 2009. Quantifying effects of simple wheat traits on yield in water-limited environments using a modelling approach. Agricultural and Forest Meteorology 149, 1095–1104.
Semenov, M.A., Stratonovitch, P., 2010. The use of multi-model ensembles from global climate models for impact assessments of climate change. Climate Research 41, 1–14.
Semenov, M.A., Shewry, P.R., 2011. Modelling predicts that heat stress, not drought, will increase vulnerability of wheat in Europe. Scientific Reports 1, 66.
Senapati, N., Brown, H.E., Semenov, M.A., 2019. Raising genetic yield potential in high productive countries: Designing wheat ideotypes under climate change. Agricultural and Forest Meteorology 271, 33–45.
Shearman, V.J., Sylvester-Bradley, R., Scott, R.K., Foulkes, M.J., 2005. Physiological processes associated with wheat yield progress in the UK. Crop Science 45, 175–185.
Shiferaw, B., Smale, M., Braun, H., Duveiller, E., Reynolds, M., Muricho, G., 2013. Crops that feed the world 10. Past successes and future challenges to the role played by wheat in global food security. Food Security 5, 291–317.
Spinoni, J., Naumann, G., Vogt, J.V., Barbosa, P., 2015. The biggest drought events in Europe from 1950 to 2012. Journal of Hydrology: Regional Studies 3, 509–524.
Sterling, M., Baker, C.J., Berry, P.M., Wade, A., 2003. An experimental investigation of the lodging of wheat. Agricultural and Forest Meteorology 119, 149–165.
Thornthwaite, C.W., 1948. An approach toward a Rational Classification of Climate. Geography Reviews 38, 55–94.
Trnka, M., Rötter, R.P., Ruiz-Ramos, M., Kersebaum, K.C., Olesen, J.E., Žalud, Z., Semenov, M.A., 2014. Adverse weather conditions for European wheat production will become more frequent with climate change. Nature Climate Change 4, 637–643.
Trnka, M., Feng, S., Semenov, M.A., Olesen, J.E., Kersebaum, K.C., Rötter, R.P., Semerádová, D., Klem, K., Huang, W., Ruiz-Ramos, M., Hlavinka, P., 2019. Mitigation efforts will not fully alleviate the increase in water scarcity occurrence probability in wheat-producing areas. *Science Advances* 5(9), p.eaau2406.Tunaloglu, R., Durdu, Ö.F., 2012. Assessment of future olive crop yield by a comparative evaluation of drought indices: a case study in western Turkey. Theoretical Applied Climatology 108, 397–410.
Vicente-Serrano, S.M., Beguería, S., López-Moreno, J.I., Angulo, M., El Kenawy, A., 2010. A New Global 0.5° Gridded dataset (1901–2006) of a multiscalar drought index: comparison with current drought index datasets based on the Palmer Drought Severity Index. Journal of Hydrometeorology 11, 1033–1043.
Vicente-Serrano, S.M., Beguería, S., Lorenzo-Lacruz, J., Camarero, J.J., Lopez-Moreno, J. I., Azorin-Molina, C., Revuelto, J., Moran-Tejeda, E., Sanchez-Lorenzo, A., 2012. Performance of drought indices for ecological, agricultural, and hydrological applications. Earth Interactions 16 (10).
Webber, H., Ewert, F., Olesen, J.E., Müller, C., Fronzek, S., Ruane, A.C., Bourgault, M., Martre, P., Ababaei, B., Bindi, M., Ferrise, R., 2018. Diverging importance of drought stress for maize and winter wheat in Europe. Nature Communications 9 (1), 1–10.
Wilhite, D.A., 2005. Drought and water crises: science, technology, and management issues. CRC Press, Boca Raton, Florida.
World Meteorological Organization. 2012. Standardized Precipitation Index User Guide (WMO-No. 1090). (1090): 24.
Wreford, A., Adger, W.N., 2011. Adaptation in agriculture: historic effects of heat waves and droughts on UK agriculture Adaptation in agriculture: historic effects of heat waves and droughts on UK agriculture. International Journal of Agricultural Sustainability 8, 278–289.
Zargar, A., Sadiq, R., Naser, B., Khan, F.I., 2011. A review of drought indices. Environmental Reviews 19, 333–349.